First-order instability theory for magnetostatic modes in ferromagnetic spheres

Ming Chen and Carl E. Patton
Department of Physics, Colorado State University, Fort Collins, Colorado 80523

A first-order instability theory for magnetostatic modes in ferromagnetic spheres has been developed. The analysis is based on the interaction of three modes: the uniform mode pumped at microwave frequency ω_p and a pair of magnetostatic modes at lower frequencies which sum to ω_p. The magnetostatic mode instability arises when the pump microwave field amplitude exceeds some threshold. The theory yields (i) selection rules for the magnetostatic mode pairs with a nonzero coupling to the uniform mode, (ii) a characteristic equation for the frequencies of these modes, and (iii) microwave field threshold amplitudes for the parametric excitation of the mode pairs. For each mode pair, one or more sharp threshold minima are found. The superposition of these sharp minima resembles the complicated structure observed in the subsidiary absorption butterfly curve for single-crystal yttrium-iron-garnet spheres.

I. INTRODUCTION

The first-order spin-wave instability theory developed by Suhl[1] and Schlömann[2] has been successful in accounting for microwave processes in ferrites at high power levels. However, the butterfly curve (microwave field threshold amplitude versus static external field) for the subsidiary absorption spin-wave instability process in single-crystal yttrium-iron-garnet (YIG) spheres has been found to exhibit a broad minimum with a complicated structure, which cannot be explained by the spin-wave theory.[3] Data from Ref. 3 for a narrow linewidth single-crystal YIG sphere at 9.16 GHz are shown in Fig. 1. The butterfly curve shows many dips, bumps, and kinks.

Both the conventional spin-wave instability analysis[3] and recent Brillouin light-scattering measurements[4] indicate that low-wave-number spin waves are the unstable modes in this region of the butterfly curve. In the limit of low wave numbers, the normal modes are so-called magnetostatic modes.[5,6] Various authors[7–10] have contributed to the development of an instability theory for magnetostatic (MS) modes in subsidiary absorption, but none of them provide direct and quantitative contact with experiment. The objective of this work was to develop a MS-mode instability theory for spheres. The approach is similar to that used by Suhl, but for discrete MS modes rather than continuous spin waves. The theory shows that the instability of specific MS-mode pairs arises when the pump microwave field amplitude exceeds some threshold. For each mode pair, one or more sharp threshold minima are found. The superposition of these sharp minima resembles the structure observed in the subsidiary absorption butterfly curve for single-crystal YIG spheres.

II. THEORY

The present theory is developed by extending the linear MS-mode theory by Walker[5] and Fletcher and Bell[6] to include the contributions of first-order nonlinear terms in the magnetic torque equation of motion, similar to the approach taken in the Suhl first-order instability theory for spin waves[1] and first applied to MS modes by Suhl[7] and Monosov.[8,9] The basic idea is that the uniform precession mode pumped at microwave frequency ω_p couples to a pair of MS modes at frequencies ω_1 and ω_2 which satisfy

$$\omega_1+\omega_2=\omega_p. \tag{1}$$

In the Suhl theory, ω_1 and ω_2 are limited to $\omega_p/2$. This is not the case for MS-mode instability.

These MS modes are also constrained to lie within the low-wave-number spin-wave band frequency limits ω_H and ω_B, where the ω_H and ω_B parameters are given by $\omega_H=\gamma H_i$ and $\omega_B=\gamma[H_i(H_i+4\pi M_s)]^{1/2}$. In these expressions, γ is the gyromagnetic ratio, $4\pi M_s$ is the saturation induction, and H_i is the static internal field. This constraint, in conjunction with Eq. (1), leads a limited frequency-field region for the allowed MS-mode pairs which are candidates for instability. This region can be illustrated by a so-called "magic diamond" which is formed by plotting ω_B, ω_H, $\omega_p-\omega_B$, and $\omega_p-\omega_H$ versus field. Such a plot is shown in Fig. 2. In the figure, the horizontal axis shows static external field, which is related to H_i by the equation $H_{\rm ext}=H_i+4\pi M_s/3$. The magic diamond is formed by the intersection of the four branches in the figure.

The present theory leads to basic selection rules for the mode pairs which may be coupled to the uniform precession mode at ω_p. These selection rules are based on the form of the scalar potential functions of the linear MS modes in the Walker–Fletcher–Bell (WFB) theory,

$$\Psi_{n,m}(\omega)=P_n^m(\xi)P_n^m(\cos\eta)e^{-im\phi}. \tag{2}$$

The P_n^m are the associated Legendre functions and (ξ,η,ϕ) represent transformed spheroidal coordinates defined in the WFB theory.[6] The $\Psi_{n,m}(\omega)$ scalar potential functions are termed "Walker-form" modes. For two Walker-form modes with indices (n_1,m_1) and (n_2,m_2), the selection rule is given by

$$n_1=n_2, \tag{3a}$$

and

$$m_1=1-m_2. \tag{3b}$$

 0021-8979/91/085724-03$03.00 © 1991 American Institute of Physics

Downloaded 26 Dec 2001 to 129.82.140.114. Redistribution subject to AIP license or copyright, see http://ojps.aip.org/japo/japcr.jsp

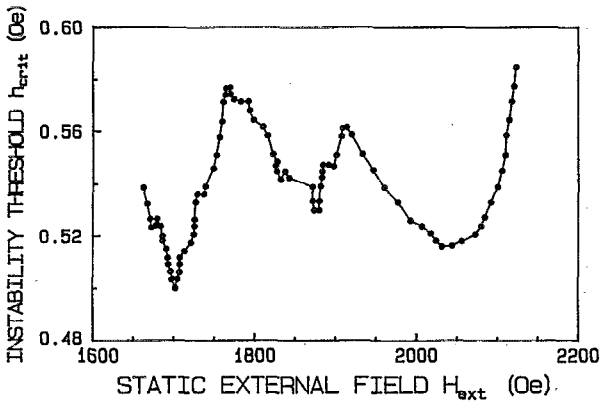

FIG. 1. Data on the instability threshold microwave field amplitude h_{crit} vs static external field H_{ext} over the low-wave-number region of the subsidiary absorption butterfly curve for a single-crystal YIG sphere at 9.16 GHz (after Patton and Jantz, Ref. 3).

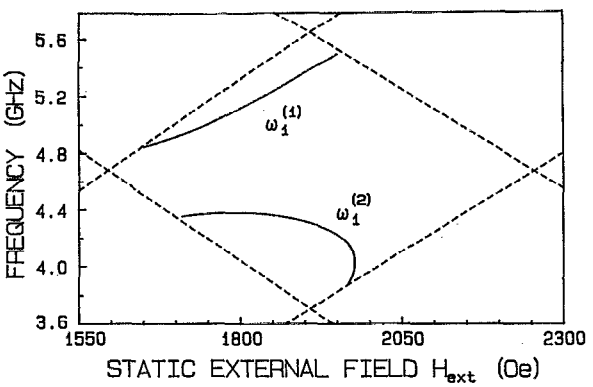

FIG. 3. Branch frequency solutions $\omega_1^{(1)}$ and $\omega_1^{(2)}$ vs static external field H_{ext} for the [(2,1), (2,0)] MS-mode pair. The solutions are limited in frequency and field to the magic diamond region formed by the dashed lines.

The detailed theory is straightforward but tedious. One obtains scalar potential solutions for a given nonlinear mode pair $[(n_1,m_1), (n_2,m_2)]$ above threshold. By incorporating these solutions into the usual boundary value problem, one obtains a secular equation of the form

$$F_1(\omega_1)F_2^*(\omega_2) - (\alpha_0^+/2)^2 F_3(\omega_1,\omega_2)F_4^*(\omega_1,\omega_2)=0. \quad (4)$$

The $F_1(\omega_1)$, $F_2(\omega_2)$, $F_3(\omega_1,\omega_2)$, and $F_4(\omega_1,\omega_2)$ functions are complicated but tractable functions of the P_n^m functions and related parameters. In Eq. (4), α_0^+ denotes the uniform mode Larmor response, which scales with the microwave pump field amplitude h,

$$\alpha_0^+ = \gamma h/(\gamma H_{ext} - \omega_p). \quad (5)$$

In order to take damping into account, ω_1 and ω_2 in Eq. (4) are replaced by complex frequencies Ω_1 and Ω_2,

$$\Omega_{1,2}=\omega_{1,2} + i\gamma\Delta H/2, \quad (6)$$

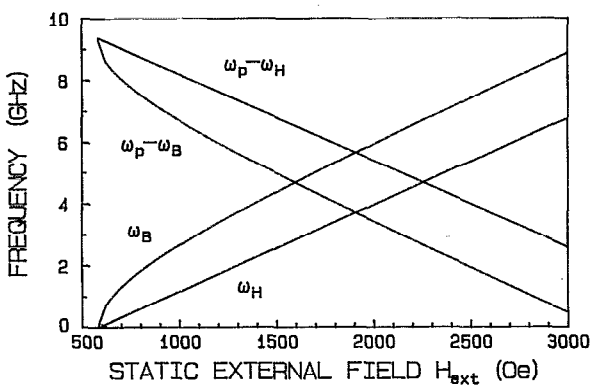

FIG. 2. Low-wave-number spin-wave frequency band limits ω_H, ω_B, $\omega_p - \omega_H$, and $\omega_p - \omega_B$ vs static external field H_{ext}. A "magic diamond" is formed in the central region of the figure by the intersection of the four branches.

where ΔH denotes the MS-mode linewidth. Subject to the small linewidth condition, $\gamma\Delta H/2 \ll \omega_{1,2}$, the imaginary part of Eq. (4) yields

$$(\partial F_1/\partial\omega_1)F_2 - (\partial F_2/\partial\omega_2)F_1=0. \quad (7)$$

Equation (7) constitutes a characteristic equation which, in conjunction with Eq. (1), determines the frequencies $\omega_1^{(i)}$ and $\omega_2^{(i)}$.

The real part of Eq. (4) yields a threshold condition

$$(\alpha_0^+)^2=\left.\frac{4F_1F_2 + (\partial F_1/\partial\omega_1)(\partial F_2/\partial\omega_2)(\gamma\Delta H)^2}{F_3F_4}\right|_{\omega_1^{(i)},\omega_2^{(i)}}. \quad (8)$$

Equation (8), in conjunction with Eq. (5), yields explicit values for the threshold microwave field amplitude $h = h_{crit}$ for the instability of a given $[(n_1,m_1,\omega_1^{(i)}), (n_2,m_2,\omega_2^{(i)})]$ mode pair.

III. NUMERICAL RESULTS

Numerical results were obtained for the ten allowed MS-mode pairs with indices $n_1 = n_2 \leqslant 5$. The calculations were done for YIG parameters with $\gamma = 2.8$ MHz/Oe, $4\pi M_s = 1750$ G, and $\Delta H = 0.2$ Oe. Representative results for the mode pair with $n_1 = n_2 = 2$ and $m_1 = 1$ — $m_2 = 1$ are presented below. This is the lowest-order mode pair which satisfies the selection rules and is allowed in the linear theory.

Figure 3 shows the solutions of Eq. (7) for frequency ω_1 inside the magic diamond. Two solution branches are found for this lowest-order [(2,1), (2,0)] mode pair. There are ω_1 solutions which extend outside the magic diamond, but these solutions do not correspond to allowed MS modes. The mode frequency ω_2 has two companion branches to $\omega_1^{(1)}$ and $\omega_1^{(2)}$ which are given by $\omega_2^{(1)} = \omega_p - \omega_1^{(1)}$ and $\omega_2^{(2)} = \omega_p - \omega_1^{(2)}$.

With these mode frequency solutions in hand, the thresholds h_{crit} can be found from Eq. (8). In Fig. 4, these h_{crit} values corresponding to the two-frequency branches in

Downloaded 26 Dec 2001 to 129.82.140.114. Redistribution subject to AIP license or copyright, see http://ojps.aip.org/japo/japcr.jsp

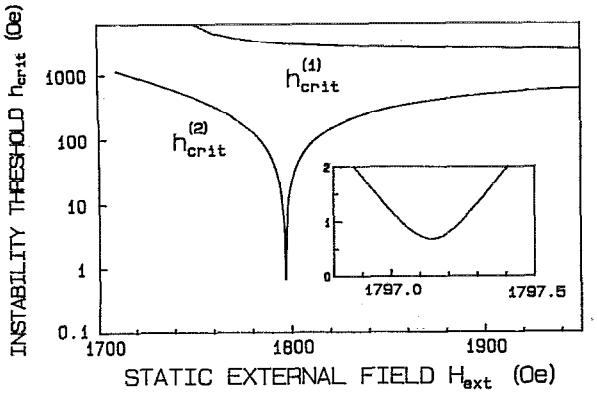

FIG. 4. Instability threshold solutions $h^{(1)}_{crit}$ and $h^{(2)}_{crit}$ vs static external field H_{ext} for the [(2,1), (2,0)] MS-mode pair. The vertical scale is logarithmic. The insert shows the dip region on an expanded linear scale.

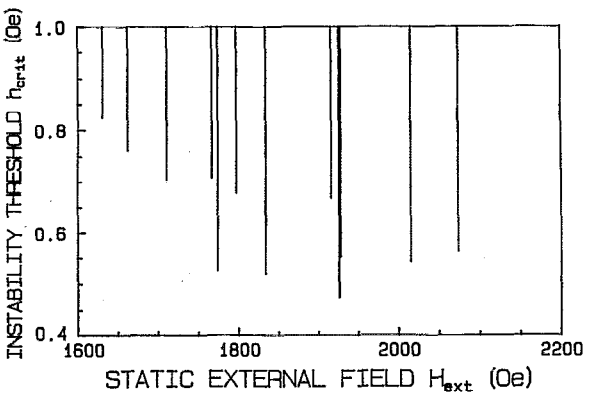

FIG. 5. Instability threshold h_{crit} vs static external field H_{ext} for the dip regions for 13 low-order ($n_1 < 5$) MS-mode pair h_{crit} solutions.

Fig. 3 are shown as a function of static external field H_{ext}. Note that the scale of the vertical axis is logarithmic. The curve for $h^{(1)}_{crit}$ is relatively flat and at very high microwave field amplitude values in excess of 1000 Oe.

The curve for $h^{(2)}_{crit}$ shows threshold values which are more reasonable and dip down into the 1-Oe range near the minimum. This branch solution exhibits a low minimum threshold of 0.6 Oe at $H_{ext} = 1797.15$ Oe. The dip associated with this minimum is very sharp and is due to the narrow linewidth used for the MS modes. Such a narrow linewidth is consistent with both the measured ferromagnetic resonance linewidth and spin-wave linewidths in the limit of low wave number. The present theory contains no adjustable parameters other than ΔH. It is noteworthy that the theory yields h_{crit} values which are comparable with experiment.

Similar results were obtained for the other allowed MS-mode pairs with indices $n_1 = n_2 \leqslant 5$. For each mode pair, multiple branch solutions for ω_1 versus field within the magic diamond were obtained. These branch solutions yield variously shaped h_{crit} versus field curves, some with large h_{crit} values and no dips and some with sharp dips. The dip solutions with low h_{crit} minimum values have been extracted from these results and are summarized in Fig. 5. As noted above, these numerical results were obtained without any adjustable parameters other than the MS-mode linewidth ΔH, taken as 0.2 Oe. As with the single dip in Fig. 4, these dips are very narrow. The minimum h_{crit} values are comparable to the threshold data in Fig. 1.

The h_{crit} dips in Fig. 5 are for only ten mode pairs. Higher-order mode pairs contribute additional dips which have not been considered explicitly. It is proposed that these dips, taken together, are the origin of the observed butterfly curve structure shown in Fig. 1. No one-to-one correlation between theoretical dips and the experimental data has yet been made.

IV. CONCLUSION

A first-order instability theory has been developed to study the parametric excitation of magnetostatic modes. Selection rules, a characteristic equation, and thresholds for the instability are obtained. The numerical results indicate that the theory provides a reasonable explanation for the complicated butterfly curve structure observed in subsidiary absorption experiments for single-crystal YIG.

[1] H. Suhl, J. Phys. Chem. Solids **1**, 209 (1957).
[2] E. Schlömann, J. J. Green, and U. Milano, J. Appl. Phys. **31**, 386s (1960).
[3] C. E. Patton and W. Jantz, J. Appl. Phys. **50**, 7082 (1979).
[4] W. D. Wilber, J. G Booth, C. E. Patton, G. Srinivasan, and R. W. Cross, J. Appl. Phys. **64**, 5477 (1988).
[5] R. L. Walker, Phys. Rev. **105**, 390 (1957).
[6] P. C. Fletcher and R. O. Bell, J. Appl. Phys. **30**, 687 (1959).
[7] H. Suhl, J. Appl. Phys. **28**, 1225 (1957).
[8] Y. A. Monosov, Radiotekh. Elektron. **5**, 85 (1960).
[9] Y. A. Monosov, Radiotekh. Elektron. **5**, 143 (1960).
[10] P. H. Bryant, Phys. Rev. B **39**, 4363 (1989).

Downloaded 26 Dec 2001 to 129.82.140.114. Redistribution subject to AIP license or copyright, see http://ojps.aip.org/japo/japcr.jsp